Home   Search   Collections   Journals   About   Contact us   My IOPscience

Ionization induced by protons on isolated molecules of adenine: theory, modelling and experiment

Ionization induced by protons on isolated molecules of adenine: theory, modelling and experiment

C. Champion[1], M. E. Galassi[2], P. F. Weck[3], C. Abdallah[4], Z. Francis[4,5],
M. A. Quinto[1], O. Fojón[2], R. D. Rivarola[2], J. Hanssen[2], Y. Iriki[6], A. Itoh[6]

[1]*Université Bordeaux 1, CNRS/IN2P3, Centre d'Etudes Nucléaires de Bordeaux Gradignan (CENBG), Gradignan, France*
[2]*Instituto de Física Rosario, CONICET and Universidad Nacional de Rosario, Argentina*
[3]*Department of Chemistry and Harry Reid Center for Environmental Studies, University of Nevada Las Vegas, USA*
[4]*University Saint Joseph, Faculty of Sciences, Department of Physics, Beirut, Lebanon*
[5]*The Open University, Faculty of Science, Department of Physical Sciences, Milton Keynes, United Kingdom*
[6]*Department of Nuclear Engineering, Kyoto University, Kyoto, Japan*

E-mail: champion@cenbg.in2p3.fr

Abstract. We here report a comparison between semi-empirical and theoretical predictions in terms of differential and total cross sections for proton-induced ionization of isolated adenine molecules. Whereas the first ones are provided by existing analytical models, the second ones are based on two quantum-mechanical models recently developed within the 1st Born and the continuum distorted wave approximation, respectively. Besides, a large set of experimental data is also reported for comparisons. In all kinematical conditions here investigated, we have observed a very good agreement between theory and experiment whereas strong discrepancies were reported with the semi-empirical models in particular when doubly-differential cross sections are analysed.

1. Introduction

Monte Carlo (MC) techniques have been demonstrated to be powerful tools for simulating 'event-by-event' radiation track structure at the nanometer level. In this context, it is worth noting that the success of such MC energy transport codes essentially depends on the accuracy of both the theoretical model assumptions and the physical input data used, *i.e.*, the cross sections implemented into the code for describing all the charged particle induced collisions.

Thus, in view of their potential applications in diverse fields like radioprotection, radiobiology, medical imaging and even in radiotherapy for treatment planning, numerous Monte Carlo codes have been developed, among which we distinguish the *specialized* Monte Carlo codes - usually called "track structure codes" and essentially devoted to microdosimetry simulations (see for example one of our previous works [1] and references therein) - from the *general-purpose* Monte Carlo codes which simulate the particle transport in matter for a large variety of ions (see for example EGS [2], FLUKA [3] and MCNP [4] with their different available versions). In this context, we have developed in the past a Monte Carlo code called TILDA for tracking heavy charged particles in biological matter [1] in which all the ion- and electron-induced interactions are described in details via a large set of multi-differential and total cross sections (for more details we refer the interested reader to our previous theoretical works devoted to the calculations of the electron and the ion-induced interaction cross sections in water [5-8]).

However, and although there is nowadays an increasing activity around the development of simulation codes able to address the questions of radio-induced damages, several questions are still today unresolved and numerous challenges remain in the development of Monte Carlo charged-particle track structure simulation models. Among many, one important challenging question concerns the use of water as surrogate of the biological medium arguing that this molecule is present in the cellular environment for more that 60-70% in mass (depending on the age of the patient). In this

context and aiming to assess the extent to which the predictions in terms of *macroscopic* deposited dose as well as of molecular *microscopic* damages at the DNA scale (single- and double-strand breaks, specific base lesions,...) should be dependent on the living matter description, we have recently reported a series of theoretical works dedicated to the description of the proton-induced ionization process [9-10] in a biological medium. Thus, within a *quantum-mechanical framework* - both in the 1st Born approximation with correct boundary conditions (CB1 model) and the continuum distorted wave-eikonal initial state approach (CDW-EIS model) we have provided a large set of ionization cross sections for protons impacting the different DNA constituents (bases and sugar-phosphate backbone).

In the current work, we aim to compare the theoretical predictions recently obtained for a target of adenine (in terms of differential as well as total ionization cross sections) to those provided by the existing *semi-empirical* models commonly used in a great part of the MC codes available in the literature. A large set of experimental data including doubly-, singly-differential and total ionization cross sections recently provided by Itoh and co-workers [11-12] will be also reported for comparison.

2. Quantum-mechanical approaches for describing the ionization process

In the present work, as well as those previously published, the biomolecule here considered as impacted by electrons is described via its molecular orbitals by employing the quantum chemical GAUSSIAN 03 program. Briefly, let us note that the target wave functions were computed at the Hartree-Fock level optimized at the MP2/6-31G(d) computational level, *i.e.* by including correlation calculations at the second order of perturbation theory MP2 and by using GAUSSIAN-type orbitals added to a double-zeta valence shell and polarization orbitals on non-hydrogen atoms. Total-energy calculations were then performed in the gas phase with the Gaussian 09 software at the RHF/3-21G level of theory. Furthermore, the ionization potentials (IP's) also calculated at the RHF/3-21G level have shown a very good agreement with the experiments. Finally, let us add that the effective number of electrons relatively to any atomic component of each molecular orbital was derived from a standard Mulliken population analysis.

Under these conditions, the target molecule ionization cross sections - whatever their degree of differentiation - were seen as a linear combination of atomic cross sections corresponding to the different component of the investigated target (H, C, N) weighted by the effective occupation electron number, namely

$$\sigma = \sum_{j=1}^{N} \sigma_j = \sum_{j=1}^{N} \sum_{i}^{N_j} \xi_{j,i} \cdot \sigma_{at,i} \qquad (1)$$

where *N* refers to the number of molecular orbitals of the impacted bio-molecule (*N* = 35 for adenine), while N_j denotes the total number of atomic components of the *j*-molecular orbital and $\sigma_{at,i}$ the corresponding atomic orbital cross sections involved in the present LCAO description (for more details, we refer the interested reader to our previous work [10]).

Finally, let us also remind that an independent active electron approximation was employed, which consists in considering the non-ionized *passive* target electrons as frozen in their initial orbitals during the collision process, as generally assumed to overcome the difficulty of taking into account the dynamical correlation between active and passive electrons in particular for large molecules like that here investigated. Thus, within this approximation, the interaction between the projectile and the passive electrons only affects the trajectory of the incident particle. Consequently, its contribution to the ionization reaction itself is neglected, which is independent of the quantum approximation used for describing the ion-induced ionization process of atoms and molecules, all the more that we here only consider calculations of cross sections integrated over the projectile scattering angle. Under these conditions, we focus in the following on the theoretical description of the dynamics of the active electron. In the sequel, we briefly outline the main features of the two quantum-mechanical models recently developed for describing the ionization process on DNA components (for more details see [9,10]).

2.1.   Ionization description within the CDW-EIS framework

In the CDW-EIS model, the initial and final distorted wave functions are chosen as

$$\chi_\alpha^+ = \frac{\exp(i\boldsymbol{K}_\alpha.\boldsymbol{R})}{(2\pi)^{3/2}}\phi_\alpha(\boldsymbol{x})\exp\left[-i\frac{Z_P}{v}\ln(vs+\boldsymbol{v}.\boldsymbol{s})\right] \tag{2}$$

and

$$\chi_\beta^- = \frac{\exp(i\boldsymbol{K}_\beta.\boldsymbol{R})}{(2\pi)^{3/2}}\phi_\beta(\boldsymbol{x})N^*(Z_T^*/k)_1F_1(-iZ_T^*/k;1;-ikx-i\boldsymbol{k}.\boldsymbol{x})$$

$$\times N^*(Z_P/p)_1F_1(-iZ_P/p;1;-ips-i\boldsymbol{p}.\boldsymbol{s}), \tag{3}$$

where the vectors $\boldsymbol{x}$ and $\boldsymbol{s}$ give the positions of the active electron with respect to the center of mass of the residual target and to the projectile, respectively, while $\boldsymbol{R}$ denotes the position of the projectile with respect to the center of mass of the target.

In Eqs.(2-3), $\boldsymbol{k}$ denotes the momentum of the ejected electron seen from the target, $\boldsymbol{p}=\boldsymbol{k}-\boldsymbol{v}$ the momentum of this electron with respect to the projectile, and $\boldsymbol{K}_\alpha$ and $\boldsymbol{K}_\beta$ the momenta of the reduced particle of the complete system in the entry and exit channels, respectively, Z_P being the projectile charge and Z_T^* an effective target charge. $N^*(a)$ refers to the conjugate of the quantity $N(a)=\exp(\pi a/2)\Gamma(1-ia)$. Besides, in Eq.(2), $\phi_\alpha(\boldsymbol{x})$ describes the bound electron wave function while the multiplicative projectile eikonal phase indicates that the active electron moves simultaneously in a bound state of the target and implicitly in a projectile eikonal continuum one. In the exit channel (see Eq.(3)), $\phi_\beta(\boldsymbol{x})$ is a plane wave that multiplied by the effective Coulomb continuum factor gives the continuum of the ionized electron in the field of the residual target while the inclusion of a multiplicative projectile continuum factor indicates that the electron is moving in a continuum state of the residual target and projectile combined fields, both considered on equal footing. Thus, initial and final distorted wave functions in CDW-EIS are chosen as two-center ones in the sense that the active electron is considered to feel the simultaneous presence of the projectile and residual target potentials in the entry and exit channels at all distances between aggregates.

Finally, let us note that the CDW-EIS treatment includes in both the initial and final distorted wave functions the long range Coulomb character of the interaction of the active electron with the projectile in the entry channel and also with the residual target in the exit one, so that they satisfy correct asymptotic conditions in both channels.

2.2. Ionization description within the CB1 framework
In the CB1 model, the initial and final wave functions are chosen as

$$\varphi_\alpha^+ = \frac{\exp(i\boldsymbol{K}_\alpha.\boldsymbol{R})}{(2\pi)^{3/2}}\phi_\alpha(\boldsymbol{x})\exp\left[-i\frac{Z_P}{v}\ln(vR-\boldsymbol{v}.\boldsymbol{R})\right] \tag{4}$$

and

$$\varphi_\beta^- = \frac{\exp(i\boldsymbol{K}_\beta.\boldsymbol{R})}{(2\pi)^{3/2}}\phi_\beta(\boldsymbol{x})N^*(Z_T^*/k)_1F_1(-iZ_T^*/k;1;-ikx-i\boldsymbol{k}.\boldsymbol{x})$$

$$\times\exp\left[+i\frac{Z_P}{v}\ln(vR+\boldsymbol{v}.\boldsymbol{R})\right] \tag{5}$$

Let us note that the main difference between the initial wave function described by Eq.(4) and that given in the CDW-EIS approach resides in an eikonal phase depending on R instead of s, so that the asymptotic boundary conditions associated with the projectile-active electron interaction are now preserved but φ_α^+ presents a one-target center character. In the exit channel (see Eq.(5)), an asymptotic version of this interaction is also considered (depending again on R), which will be valid under the dynamic condition $k << v$ ($x << R$). So, in the CB1 approximation for ionization, correct boundary conditions are only satisfied in this restricted coordinate space region. Thus, φ_β^- presents also a one-target center character. Finally, note that in the present quantum mechanical calculations, the effective target charge Z_T^* is taken as $Z_T^*=\sqrt{-2n_\alpha^2\varepsilon_\alpha}$ where n_α refers to the principal quantum number of

each atomic orbital component used in each MO expansion whereas the active electron orbital energy ε_α is related to the ionization energies B_j of the occupied molecular orbitals by $\varepsilon_\alpha = -B_j$. Each molecular orbital is thus described by using a basis of effective atomic ones.

3. Semi-empirical approaches for describing the ionization process

Due to their relative complexity as well as their big requests in terms of computing time, quantum mechanical ionization models were in the past generally put aside in the profit of semi-empirical models which offered useful parameterizations of singly-differential and total ionization cross sections (SDCS and TCS, respectively).

Among them, let us first cite the Rudd's model [13] initially developed for protons impacting atomic and molecular targets (including water). The latter provides an analytic equation for the energy distribution of electrons by means of a large set of fitting parameters deduced from experimental comparisons. It is based on a simple version of the binary-encounter approximation equation modified to yield the correct high-energy asymptotic dependence on energy in agreement with the Bethe equation prediction and further modified by the use of the promotion model at low energies. In brief, the approximation made consists in treating the collision - between a projectile and a single target electron - as a classical one. The nucleus and the remaining target electrons play no rôle except that of providing a binding energy for the ejected electron, the energy transfer E and the kinetic energy E_e being related by $E = E_e + I$, where I denotes the binding energy of the ionized subshell of the target. The justification for using a classical model lies in the fact that doubly differential cross sections for Coulomb scattering between two particles are the same when calculated using either classical physics or quantum mechanics. Thus, for each molecular subshell, the singly-differential cross sections were simply expressed as (in atomic units)

$$\frac{d\sigma_{Rudd}}{dE_e} = \frac{S/I}{2R} \frac{F_1 + F_2 w}{(1+w)^3 [1 + \exp(\alpha(w - w_c)/v)]}, \tag{6}$$

where R denotes the Rydberg energy while the reduced quantities w and v are given by

$$w = E_e / I \text{ and } v = \sqrt{E_i / I}, \tag{7}$$

where E_i denotes the incident projectile energy and with

$$w_c = 4v^2 - 2v - 1/8I \text{ and } S = \pi N / I^2, \tag{8}$$

N being the number of target electrons for each ionized molecular subshell whereas F_1, F_2 and α are seen as adjustable fitting parameters. Thus, we have

$$F_1(v) = L_1 + H_1 \text{ with } \begin{cases} L_1 = C_1 v^{D_1} / [1 + E_1 v^{(D_1+4)}] \\ H_1 = A_1 \ln(1 + v^2) / (v^2 + B_1 / v^2) \end{cases} \tag{9}$$

and

$$F_2(v) = L_2 H_2 / (L_2 + H_2) \text{ with } \begin{cases} L_2 = C_2 v^{D_2} \\ H_2 = A_2 / v^2 + B_2 / v^4. \end{cases} \tag{10}$$

Besides, the original Rudd version including not the parameters needed for describing the ionization of DNA components, Abdallah and Francis (private communication) have recently tested a large set of fitting parameters in order to reproduce the experimental cross sections reported by Iriki *et al.* on adenine [12-13]. The latter are used in the current work (see Table 1).

Total ionization cross sections were finally simply deduced by numerical integration of Eq.(6) over the kinetic energy transfers E_e, the latter ranging from a minimum value $(E_e)_{min} \cong 0$ to a maximum value $(E_e)_{max} = \frac{4m_0 M_P}{(M_P + m_0)^2} E_i \cong \frac{4m_0}{M_P} E_i$ where m_0 and M_P refer to the electron and projectile mass (given in units of electron mass), respectively.

Table 1. Rudd's model parameters for fitting the SDCS of proton-induced ionization of isolated adenine molecules (Abdallah and Francis, private communication).

	Inner shells	Outer shells
A_1	1.25	1.18
B_1	0.5	14
C_1	1	0.36
D_1	1	0.52
E_1	3	3
A_2	1.1	0.9
B_2	1.3	4.3
C_2	1	1.8
D_2	0	1.4
α	0.66	0.61

The second semi-empirical and well-documented model - called HKS model since developed by Hansen, Kocbach and Stolterfoht [14] - consists in describing the ionization process within the impact parameter 1st Born approximation. In this approach, the initial and the final electron states are described by means of a hydrogenic function and a plane wave, respectively, *i.e.* without taking into account the electron momentum in its bound state. However, due to singularities observed when the ejected electron energy tends to zero, further empirical fittings were employed to finally provide the well-known HKS model. The doubly-differential cross sections (DDCS) for each molecular subshell were then expressed as [14]

$$\frac{d^2\sigma_{HKS}}{d\Omega_e dE_e} = \frac{32N}{3\pi\alpha k_c^3 v_i^2}\left[\frac{\alpha_c^2}{\alpha_c^2 + (\hat{K}_m - \hat{k}_t\cos\theta_e)^2}\right]^3,\qquad(11)$$

where the function in the square brackets describes the binary-encounter maximum that resembles a Lorentzian whose width is governed by

$$\alpha_c = \alpha\left(1.0 + 0.7\frac{v_i^2}{v_i^2 + k_e^2}\right),\qquad(12)$$

where $\alpha = \sqrt{2I}$ corresponds to the mean initial momentum parameter, with I and N as defined above.

In Eqs.(11-12), v_i denotes the projectile velocity while $\hat{K}_m = \dfrac{K_m}{\alpha_c}$ represents the normalized minimum momentum transfer with $K_m = (\alpha^2 + k_e^2)/2v_i$. Similarly, the quantity $\hat{k}_t = k_t/\alpha_c$ and k_c - defined as small modifications of the momentum of the outgoing electron k_e - are respectively given by

$$k_t = \left[k_e^2 + 0.2\alpha^2\sqrt{v_i/\alpha}\right]^{1/2} \text{ and } k_c = \left[k_e^2 + 2\alpha^2/\ln(2v_i^2/\alpha^2)\right]^{1/2}.\qquad(13)$$

Let us note that the original equations proposed by Hansen and Kocbach [14] imply $k_c = k_e$ due to the fact that in the peaking approximation one neglects the mean momentum of the bound electrons in comparison to that of the outgoing electron. However, as clearly emphasized by Stolterfoht *et al.* [16], this approximation produces a singularity in the low-electron energy regime, which can be simply removed by adjusting the value of k_c to fit the model results to those of the Born approximation. To do that, numerous expressions have been proposed like that reported in Eq.(13). We can also mention that reported in [16], namely,

$$k_c = \left[k_e^2 + \frac{3\alpha^2/2}{[\ln(2v_i^2/\alpha^2)]^{2/3}}\right]^{1/2}.\qquad(14)$$

5

In the same state of mind, Bernal and Liendo [17-18] have recently slightly modified the original version of the HKS model, essentially to avoid the "non-physical" descending jump appearing for each electron binding energy in the SDCS due, in major part, to the use of the arctangent term (see Eq.(16)). To do that, the authors proposed a modified expression for the DDCS, denoted in the following $\left[\dfrac{d^2\sigma_{HKS}}{d\Omega_e dE_e} \right]_{BL}$ and expressed as

$$\left[\frac{d^2\sigma_{HKS}}{d\Omega_e dE_e} \right]_{BL} = \frac{32N}{3\pi\alpha k_c^3 v_i^2} \left[\frac{1}{1+(\hat{K}_m + \hat{k}_t \cos\theta_e)^2} \right]^3. \tag{15}$$

However, as underlined by Bernal and Liendo [17-18], the DDCS obtained show only limited agreement with the experimental data, especially in the backward and forward angle regions; this could stem from the use, in this model, of hydrogenic wave functions instead of realistic bound electron wave functions to describe the target electron initial state.

Furthermore, the semi-empirical SDCS provided by the different existing HKS approaches, namely, the original version $\dfrac{d\sigma_{HKS}}{dE_e}$ and the recently modified version $\left[\dfrac{d\sigma_{HKS}}{dE_e} \right]_{B-L}$ may be respectively recast as

$$\begin{aligned}
\frac{d\sigma_{HKS}}{dE_e} = \frac{16N}{3\alpha k_c^3 \hat{k}_t v_i^2} &\left[\arctan\left(\frac{2\hat{k}_t}{1+\hat{K}_m^2-\hat{k}_t^2} \right) \right. \\
&\left. + \frac{5(\hat{K}_m+\hat{k}_t)+3(\hat{K}_m+\hat{k}_t)^3}{2[1+(\hat{K}_m+\hat{k}_t)^2]^2} - \frac{5(\hat{K}_m-\hat{k}_t)+3(\hat{K}_m-\hat{k}_t)^3}{2[1+(\hat{K}_m-\hat{k}_t)^2]^2} \right]
\end{aligned} \tag{16}$$

and

$$\begin{aligned}
\left[\frac{d\sigma_{HKS}}{dE_e} \right]_{BL} = \frac{8N}{\alpha k_c^3 \hat{k}_t v_i^2} &\left[\frac{5(\hat{K}_m+\hat{k}_t)+3(\hat{K}_m+\hat{k}_t)^3}{3[1+(\hat{K}_m+\hat{k}_t)^2]^2} - \frac{5(\hat{K}_m-\hat{k}_t)+3(\hat{K}_m-\hat{k}_t)^3}{3[1+(\hat{K}_m-\hat{k}_t)^2]^2} \right. \\
&\left. + \arctan(\hat{K}_m+\hat{k}_t) - \arctan(\hat{K}_m-\hat{k}_t) \right],
\end{aligned} \tag{17}$$

Finally, we considered the simple approach provided by the Rutherford formula - and more precisely the extension provided by Thomson [19] - who presented the following analytical expression of the SDCS (per molecular subshell)

$$\left[\frac{d\sigma}{dE_e} \right] = \frac{\pi}{(E_i / M_p)} \cdot \frac{N}{(E_e + I)^2}, \tag{18}$$

where the quantities used are similar to those defined above.

However, despite its fundamental importance, the Rutherford formula noticeably underestimates the electron production cross sections at low electron energies. Thus, as pointed out by Stolterfoht *et al.* [16], the soft collision electrons are produced in dipole-type transitions and should be treated via a quantum mechanical approach. Thus, to enhance the low-energy electrons due to dipole transitions, Stolterfoht *et al.* suggested to modify the original formula (see Eq.(18)) by introducing an adjustable parameter *c* in the denominator, namely

$$\left[\frac{d\sigma}{dE_e} \right] = \frac{\pi}{(E_i / M_p)} \cdot \frac{N}{(E_e + cI)^2} \quad \text{with} \quad c = \left[\ln\left(\frac{2E_i / M_p}{I} \right) \right]^{-1/2}. \tag{19}$$

To conclude, let us note that for all these semi-empirical models, the total ionization cross sections were numerically obtained by integration of the SDCS and summation over all the subshell contributions.

Besides, let us mention that prior to the here-mentioned quantum mechanical models, we have also proposed a classical description of the ionization of the DNA components based on a CTMC-COB (for classical trajectory Monte Carlo-classical over barrier) approach [20]. In all cases a good agreement

was reported for the total ionization cross sections in comparison to the current theoretical predictions provided that the impact energy remains greater than about 100 keV.

Finally, let us mention the recent study of de Vera *et al.* [21] where a semi-empirical model was used for calculating the electron emission from any organic compound after ion impact. With only the input of the density and composition of the target the authors provided SDCS in very good agreement with the experiment.

4. Results and discussion

In Figure 1 we compare our calculated total ionization cross sections to the rare existing experimental data, namely, the measurements provided by Tabet *et al.* [22] for 80keV-protons (solid circle) and those recently reported by Iriki *et al.* [11,12] for three higher energies, namely, 500 keV, 1 MeV and 2 MeV (solid triangles). It clearly appears that the 1st Born as well as the CDW-EIS results (green and dark cyan line, respectively) exhibit a very good agreement with the recent measurements, while a large disagreement is observed for the lowest impact energy investigated. This divergence remains still today not understood all the more the CDW-EIS model should provide accurate results at this energy of 80 keV. Besides, let us note that the CB1 data tend to largely overestimate the majority of the other models for incident energies lower than about 60-70 keV. In this context, it is worth noting that further experiments are crucially needed to check the currently developed quantum-mechanical models. In the same way, let us note that the classical description reported by Lekadir *et al.* [20] (dark yellow line) also exhibits a good agreement with the quantum mechanical predictions provided that the proton energy remains greater than about 200-300 keV. Finally, we observe that the semi-empirical models here tested exhibit an overall good agreement, in particular with the CDW-EIS model, except for the Rutherford and the Rudd models (orange and cyan line, respectively) as well as the HKS model modified by Stolterfoht *et al.* [16] (blue line). On the contrary, the original version of the HKS model as well as that proposed by Bernal and Liendo [17,18] (red and magenta line, respectively) exhibit a very good agreement with the CDW-EIS predictions over the entire energy range.
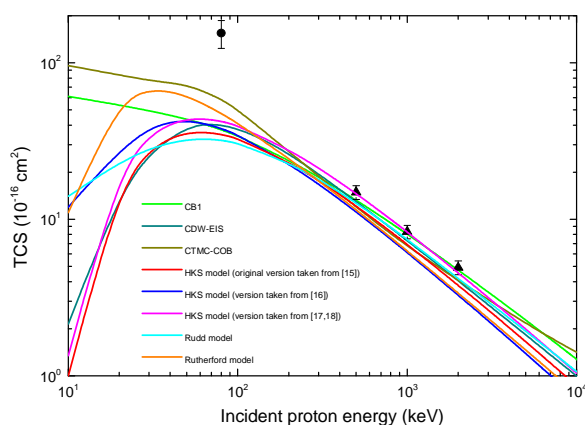

Figure 1. Total ionization cross sections of adenine.
Comparison between theoretical and semi-empirical models as
well as experimental data [11,12,22] (in all cases the error bars
are of about 10%).

Similarly, we report in Figure 2 a comparison of the experimental SDCS provided by Itoh and co-workers for the three energies studied, namely, 500 keV, 1 MeV and 2 MeV, with the different models here investigated, theoretical as well as semi-empirical. Thus, we clearly observe that the singly-differential cross sections fit very well the experiment over the entire range of ejected energies. Nevertheless, we note that the low-energy domain of ejected energies remains largely overestimated by all the models, with in particular a strong disagreement - of one order of magnitude - at $E_e = 1$ eV. However, it is worth noting that experimental errors may be also very important in this domain (Itoh, private communication).
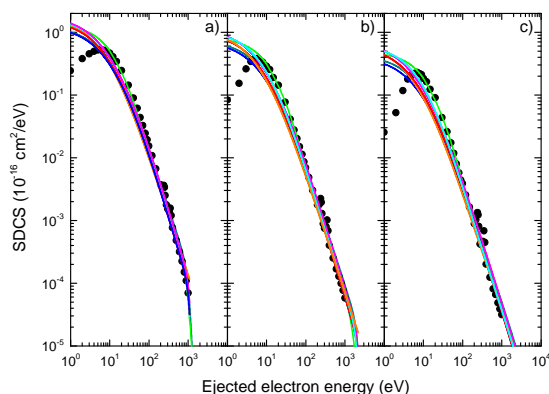
Figure 2. Singly-differential ionization cross sections of
adenine. Comparison between theoretical and semi-empirical
models as well as experimental data for three incident energies
[11,12]: a) $E_i = 500$ keV, b) $E_i = 1$ MeV and c) $E_i = 2$ MeV (in
all cases the error bars are of about 10%). Same colours as in
Figure 1 are used.

Finally, we report in Figure 3 the angular distributions of the ejected electrons for an incident
energy of 2 MeV and for particular ejection directions, namely, $\theta_e = 15°$, $45°$, $75°$, $105°$, $135°$ and
$165°$. The best agreement is obtained with the CB1 model (green line), which reproduces very well the
experiment over the whole ejected energy range, except once again in the very low-energy regime
($E_e < 10$ eV). In the same way, the CDW-EIS predictions (dark cyan line) appear in good agreement
with the experimental data, except for the backward direction, which is, as expected, largely
underestimated. Finally, regarding the different HKS model versions, we observe that they show an
overall good agreement with minor discrepancies between each other, in particular the original HKS
version (red line) and that suggested by Stolterfoht *et al.* (blue line). Indeed, from Fig.3, it clearly
appears that the semi-empirical predictions provided by the version proposed by Bernal and Liendo
(magenta line) largely underestimate the experimental data, all the more the ejected energy increases
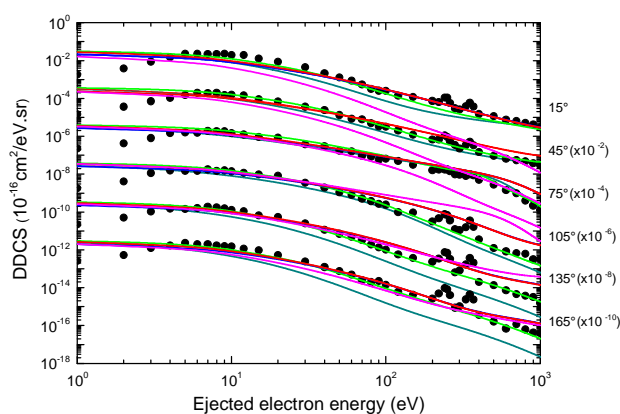and more pronounced in the forward directions.

Figure 3. Doubly-differential ionization cross sections of
adenine. Comparison between theoretical and semi-empirical
models as well as experimental data for 2 MeV incident protons
reported as a function of the ejected electron energy at fixed
ejection directions [11,12] (error bars of about 15%). Scaling
factors reported in parenthesis were used for clarity reasons.
Same colours as in Figure 1 are used.

5. Conclusions

We have investigated in the current work theoretical calculations of doubly, singly and total ionization cross sections of isolated adenine molecules impacted by proton beams. Our *ab initio* models - CB1 as well as CDW-EIS - reproduce with a very good agreement the existing experimental measurements. In this context, the CB1 model has clearly demonstrated its ability to describe in details the DNA macromolecule ionization by highly energetic protons. Besides, in comparison to the semi-empirical models, it has been shown that some of them were unable to reproduce with the same degree of accuracy the experiment, in particular when the most differential cross sections were studied.

6. References

[1]   Champion C, L'Hoir A, Politis M F, Fainstein P D, Rivarola R D and Chetioui A 2005 *Radiat. Res.* **163** 222
[2]   Nelson W R, Hirayama H and Rogers D W O 1985 Stanford Linear Accelerator Center, Stanford, CA (*Tech. Rep. SLAC-265*)
[3]   Ferrari A, Sala P R, Fassò A and Ranft J 2005 CERN, Geneva, Switzerland (*Tech. Rep. CERN-2005-010, INFN/TC-05/11, SLAC-R-773*)
[4]   X-5 Monte Carlo Team 2003 Los Alamos National Laboratory, Los Alamos, NM (*Tech. Rep. LA-UR-03-1987*)
[5]   Champion C 2003 *Phys. Med. Biol.* **48** 2147
[6]   Boudrioua O, Champion C, Dal Cappello C and Popov Y V 2007 *Phys. Rev.* A. **75** 022720
[7]   Champion C, Boudrioua O, Dal Cappello C, Sato Y and Ohsawa D 2007 *Phys. Rev.* A. **75** 032724
[8]   C. Dal Cappello, C. Champion, O. Boudrioua, H. Lekadir, Y. Sato and D. Ohsawa 2009 *Nucl. Instrum. Methods Phys. Res., Sect.* B **267** 781
[9]   Champion C, Lekadir H, Galassi M E, Fójon O, Rivarola R D and Hanssen J 2010 *Phys. Med. Biol.* **55** 6053
[10]   Galassi M E, Champion C, Weck P F, Rivarola R D, Fojón O and Hanssen J 2012 *Phys. Med. Biol.* **57** 2081
[11]   Iriki Y, Kikuchi Y, Imai M and Itoh A 2011 *Phys. Rev.* A **84** 032704
[12]   Iriki Y, Kikuchi Y, Imai M and Itoh A 2011 *Phys. Rev.* A **84** 052719
[13]   Rudd M E 1989 *Nucl. Tracks Radiat. Meas.* **16** 213
[14]   Hansen J P and Kocbach L 1989 *J. Phys.* B **22** L71
[15]   Rudd M E, Kim Y K, Märk T D *et al.* 1996 (*Technical Report 55, International Commissions on Radiation Units and Measurements*, Bethesda, MD)
[16]   Stolterfoht N, DuBois R and Rivarola R D 1997 *Electron Emission in Heavy Ion-atom Collisions* (Springer, Berlin)
[17]   Bernal M A and Liendo J A 2006 *Nucl. Instrum. Methods Phys. Res., Sect.* B **251** 171
[18]   Bernal M A and Liendo J A 2007 *Nucl. Instrum. Methods Phys. Res., Sect.* B **262** 1
[19]   Thomson J J 1912 *Phil. Mag.* **23** 449
[20]   Lekadir H, Abbas I, Champion C, Fojón O, Rivarola R and Hanssen J 2009 *Phys. Rev. A* **79** 062710
[21]   de Vera P, Garcia-Molina R, Abril I and Solov'yov A V 2013 *Phys. Rev. Lett.* **110** 148104
[22]   Tabet J, Eden S, Feil S, Abdoul-Carime H, Farizon B, Farizon M, Ouaskit S and Märk T D 2010 *Phys. Rev. A* **82** 022703